

# Path Loss Models for Low-Power Wide-Area Networks: Experimental Results using LoRa

Hendrik Linka\*, Michael Rademacher\*, Osianoh Glenn Aliu<sup>†</sup>, Karl Jonas\*

\*Hochschule Bonn Rhein-Sieg, Sankt Augustin, Germany

hendrik.linka@smail.inf.h-brs.de, michael.rademacher@h-brs.de, karl.jonas@h-brs.de

<sup>†</sup>Fraunhofer Fit, Sankt Augustin, Germany

osianoh.glenn.aliu@fit.fraunhofer.de

**Abstract**—More and more low-power wide-area networks (LPWANs) are being deployed and planning the gateway locations plays a significant role for the network range, performance and profitability. We choose LoRa as one LPWAN technology and evaluated the accuracy of the Received Signal Strength Indication (RSSI) of different chipsets in a laboratory environment. The results show the chipsets report significantly different RSSI. To estimate the range of a LPWAN beforehand, path loss models have been proposed. Compared to previous work, we evaluated the Longley-Rice Irregular Terrain Model which makes use of real-world elevation data to predict the path loss. To verify the results of that prediction, an extensive measurements campaign in a semi-urban area in Germany has been conducted. The results show that terrain data can increase the prediction accuracy.

**Index Terms**—LoRa; Path loss model; LoRa receiver accuracy; Free-Space Loss (FSL); Longley-Rice Irregular Terrain Model (ITM)

## I. INTRODUCTION AND MOTIVATION

There has been a significant adoption of Internet of Things (IoT) technologies in commercial applications in a wide range of environments. Common outdoor IoT applications require a low power device that forwards the data over wide areas to a gateway. The device should operate independently a significant amount of time (magnitude of years) on batteries and not require regular maintenance to be profitable. A system with these characteristics is called a LPWAN.

In Europe, the Industrial, Scientific and Medical (ISM) band (433 MHz and 868 MHz) is mainly used for the operation of LPWAN since it does not require a spectrum license [1]. The field of application for LPWANs ranges from smart cities to environmental monitoring to industrial applications. By 2020, there will be tens of billions of smart devices [2]. Some of them must use a transmission technology that is customized to the conditions of the environment. LoRaWAN is one of many LPWAN transmission technologies. The so called LoRa modulation is based on chirp spread spectrum enhanced by forward error correction for all messages [3].

One of the most interesting properties that makes LoRa special is the ability of the sensors to forward data with energy-constrained devices over large distances. Fundamentally, transmitting data over large distances in a wireless channel requires high transmission power. However, even at 14 dBm output power, LoRa can transmit data to a distance of up to 25 km in a semi-urban area assuming line-of-sight.

There are different possible applications for the LoRa technology or LPWAN in general. One may be the detection of water levels with multiple sensors along a river. These sensors are installed far apart from each other in rural areas and measure the water level in regions located downstream [3]. In urban environments, parking sensors check whether a car is parked in a specific spot and conduct energy harvesting to extend their battery life. These sensors are especially useful in big cities where parking spaces are limited [4]. However, especially in (semi-)urban environments, the transmission can be disrupted by surrounding buildings, and a forecast for a gateway location must be generated to guarantee the correct operation of the entire system. A path-loss model may produce precise predictions by forecasting possible receive signal strengths. These predictions could be used to install the gateways at appropriate locations and guarantee the operation of the sensors.

In this work, we are testing different published path-loss models and checking their capabilities against real signal measurements from a LoRa test deployment. In addition, we contribute the evaluation of path-loss model which makes use of terrain data to enhance the predictions. We start by discussing related work and path loss models in Section II. Afterwards, a subset of models is selected and examined further in Section III. Section IV describes the measurement setup with further challenges introduced by the LoRa chipsets. In Section V, the results are analyzed and discussed. Finally, in Section VI, we summarize our results and provide ideas for possible future research directions.

## II. RELATED WORK

Table I provides an overview of significant contributions in context of evaluated path-loss models for LPWAN. In [1], the authors compare 6 majorly used path loss models to determine their accuracy. Testbeds are set up at different locations in Dortmund, Germany. The research group uses the Pycom LoPy transceiver for a range test at 433 MHz and 868 MHz. The setup consists of one gateway and eight nodes, which are spread throughout the city. Four nodes are placed indoors while the other four are installed outdoors. All nodes use a spreading factor of 12 and a coding rate of 4/8. In addition, the authors tested the 433 MHz and 868 MHz bands with a moving transceiver mounted on the roof of a car at a height of

1.7 m. The comparison of their live measurements with the 6 other path loss models shows an imprecise prediction for the real signal data. Therefore, the authors propose a new model.

The authors in [5] conduct a coverage comparison of General Packet Radio Service (GPRS), Narrowband-IoT, LoRa, and Sigfox for a  $7,947\text{-km}^2$  area with two different models that use the Danish digital height model 2007 [6] for the height of the terrain. The height model was scaled down to 100 m to decrease the computational load. The result of the calculation shows the coverage for four different technologies. However, the authors did not compare the evaluated path-loss models with real world measurements.

In [7], the authors conduct a test with a mounted LoRa transmitter on the roof of a car in city of Oulu. A second LoRa transmitter on a boat provides additional measurement data. The measured signal strengths are compared to the Free-Space Path Loss (FSPL) model. The results show a significant deviation and the authors therefore propose a new path loss model.

To the best of our knowledge, there is no work which evaluated the role of topographical data to improve the accuracy of a LPWAN path loss model.

Paper	Evaluated path-loss models
[1]	Free space path loss model Okumura Hata Model ITU-Advanced Channel Model for Urban Macro NLOS Areas Winner+ Channel Models for Urban Macro NLOS Areas 3GPP Spatial Channel Model for Urban Macro Areas Oulu channel model proposed Dortmund (urban) path loss model
[5]	3GPP Rural Macro non-line-of-sight (NLOS) model (rural areas) 3GPP Urban Macro NLOS model (urban areas)
[7]	Free space path loss model Oulu Model

TABLE I: Related work.

### III. PATH LOSS MODELS

Based on the related work presented in Section II and the survey presented in [8] we selected three different path-loss models for further evaluation. In the following, we provide a short summary of each model.

#### A. Free-Space Path Loss

The purely analytic FSPL (Friis equation [9]) model serves as a baseline in our analysis. In addition, it is an integral component of all forthcoming approaches. The equation is given in the logarithmic domain as follows:

$$PL_{fs} = 20 * \log_{10}(f) + 20 * \log_{10}(d) + 32.45 \quad (1)$$

Here and henceforth, the distance (d) is given in km, the frequency (f) in MHz and the path loss ( $PL_x$ ) is in units of decibels relative to a mW (dBm) [8].

#### B. Regression Coefficient

Based on their measurement data, the authors in [10] and [1] derived a regression curve for the mean path loss using the following equation:

$$PL_{coeff} = B + 10 * n * \log_{10}\left(\frac{d}{d_0}\right) \quad (2)$$

Using a reference distance of  $d_0 = 1 \text{ km}$ , a path loss exponent (n) and a path loss intercept (B) have been derived. In the city of Dortmund (Germany), the authors in [1] determined  $n = 2.65$  and  $B = 132.25$ . Different results have been calculated in the city of Oulu (Finland) [10], where  $n = 2.32$  and  $B = 128.95$  fitted best to the samples obtained.

#### C. Longley-Rice Irregular Terrain Model

The ITM incorporates various additional parameters to increase the accuracy of path-loss predictions like the soil condition, the climate but most importantly refraction and diffraction due to obstacles and terrain. The model is applicable from 20 MHz up to 20 GHz and has been widely used in the context of TV broadcasting. In the simplest form, the model can be stated as:

$$PL_{ITM} = PL_{fs} + A_{ref} \quad (3)$$

The component  $A_{ref}$  sums up possible attenuation in addition to the FSPL. It is computed using three different distance ranges [11]. For shorter distances, mostly at line-of-sight, the two-ray model is used. For distances where the horizon limits the line-of-sight or in the case there is an obstruction, diffraction is the dominant factor and a double knife edge estimation is applied. For very long distances, scattering becomes the dominant factor for  $A_{ref}$ . For a detailed description of  $A_{ref}$  we refer the reader to [11], [12].

The Longley-Rice Model requires terrain data for accurate diffraction computations. We found two options to obtain suitable terrain data for our area. The first option is data acquired by the Shuttle Radar Topography Mission (SRTM) in February 2000. The result of this mission is a large set of digital elevation models (DEMs) at a resolution of 1 arc second ( $\approx 30 \text{ m}$ ) between  $60^\circ N$  and  $57^\circ S$  [13]. The data is freely available online at [14]. The second option is to use data obtained by the Light detecting and ranging (LIDAR) technique. LIDAR systems obtain terrain data by evaluating the reflection of a laser beneath the flight path of an aircraft. Compared to the SRTM data, the resolution is much higher but such data is rarely available in public domain. To calculate  $PL_{ITM}$ , we use an already established software package called SPLAT available at [15]. The parameters of the Longley-Rice model are summarized in Table II.



Fig. 1: Antenna and test setup.

Earth Dielectric Constant	5.0
Earth Conductivity	0.001 [S/m]
Atmospheric Bending Constant	301
Radio Climate	5
Fraction of situations	0.9
Fraction of time	0.9

TABLE II: Longley-Rice model parameters.

#### IV. MEASUREMENT SETUP

The test was conducted at the Bonn-Rhein-Sieg University of Applied Sciences, Germany. The building is surrounded by different terrain. There is a mountain in the north of the test area. In the east lies a densely populated city and in the south is a flat rural area.

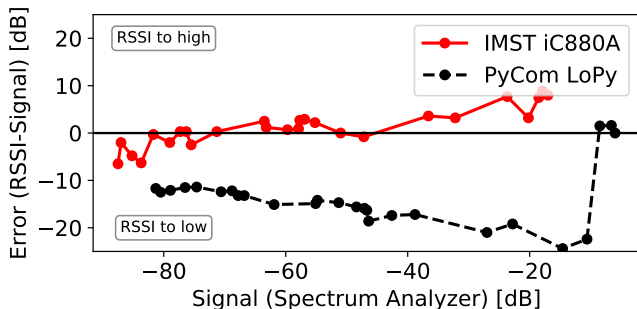


Fig. 2: Chipset RSSI accuracy verification.

##### A. Testbed

The measurement setup consists of a fixed LoRa transceiver on the roof of the university (Fig. 1a) and a moving transceiver installed on a car at a height of 1.2 m (Fig. 1b). For the fixed transceiver, we used the IMST iC880A. It features an SX1301 digital baseband chipset and two SX1257 radios for LoRa transmissions and demodulations. We installed it at a height of 22 m. The moving transmitter was placed on a car with a Global Positioning System (GPS) logger. First tests were performed with the Pycom LoPy and the PyTrack GPS

expansion board. The LoPy has an integrated LoRa SX1272 transceiver and an additional WiFi transceiver.

After quickly evaluating our first results, we decided to test the reliability of the reported RSSI value of both transceivers. For this test, we build-up a small experiment in our laboratory utilizing an industrial grade spectrum analyzer visible in Fig. 1c. The transceivers of the iC880A and the LoPy were directly connected by a 50- $\Omega$  cable. In the middle of the connection, we used fixed and dynamic attenuators to simulate the path-loss. The spectrum analyzer, connected via a splitter, measures the strength of each signal down to a noise level of -82 dB. For each attenuation setting noted the RSSI and the reported channel power by the spectrum analyzer. Fig. 2 shows the deviation (RSSI-Signal) for both transceivers.

The average deviation for the iC880A is 3.12 dB while the LoPy, has an average deviation of 13.85 dB (2). Therefore, to keep the measurement error for the path-loss model evaluation as small as possible, we decided to use two iC880A transceivers. The disadvantage of the IMST iC880A is its minimum receiving signal strength of -125 dB. We were unable to receive lower RSSI values with a fixed setting of spreading factor 12 and 125 kHz. Similar observations have already been made in [16]. The GPS measurements are still produced by the L76-L chipset of the LoPy expansion board. The GPS chipset has an accuracy of less than 2.5 m Circular Error Probable (CEP) [17]. A test with a geodetic measuring point delivered a deviation of 4 m which is a sufficient accuracy for our use-case.

##### B. Acquisition of data

After the receiver performance of the LoRa and GPS chipsets was reviewed, ten points surrounding the university were selected. Besides the measurements of these points, we recorded the paths between them. The transmitted LoRa messages had a size of 11 bytes. We used a spreading factor of 12 to maximize the range. In addition, the coding rate was 4/5 with a bandwidth of 125 kHz. We used a fixed channel at 868.1 MHz. At the end of the experiment, three tables were generated with synchronized time stamps. One table contains the GPS positions of the car, which are rounded to  $10^{-3}$  decimal degrees ( $\approx 11$  m). The second table includes

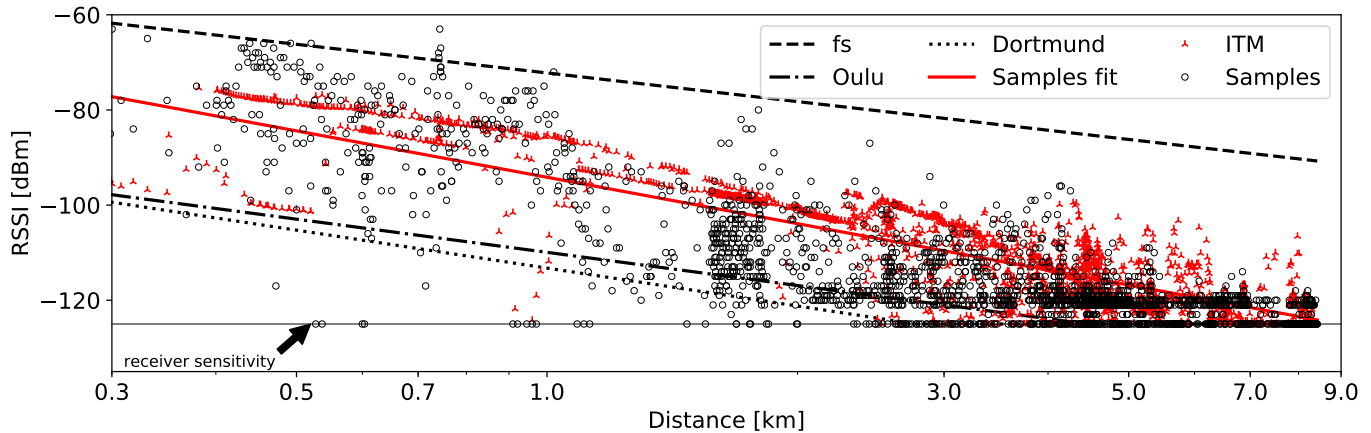


Fig. 3: Results for different evaluated path loss models and our field measurements.

the sent LoRa messages, and the third table includes the received LoRa messages with their signal strength. By merging these tables, a table of GPS locations and signal strength is created. Furthermore, lost signals are included, along with the GPS locations of the car. If multiple measurements exist for one location ( $10^{-3}$  decimal degrees), the mean value of these measurements is used to account for different fading effects. Lost signals which occurred between two valid LoRa transmissions are considered interference/collisions and are removed from the data-set. For the uplink (the transmission from the node to the gateway), 3,745 different measurements were collected. The downlink data-set has a size of 3,819 different measurements.

After the aggregation of data, predictions for the surrounding area of the University were generated. The equivalent isotropically radiated power (EIRP) is set to 17 dB. This value consists of 14 dB transmit power and an additional 5 dBi of antenna gain. For the 5 m cable attached to the car antenna, we subtract 2 dB. Due to the high computing power required by the uplink for terrain models, we evaluate only the downlink in this work.

## V. RESULTS AND ANALYSIS

In Fig. 3, we compare the distance of the car to the gateway with the measured RSSI samples. In addition, we added the four models described in Section III. All predicted values below -125 dBm were mapped to the maximum receiver sensitivity of -125 dBm for a more meaningful comparison.

The values predicted by the FSPL model are as expected above the samples with a few outliers which we assume are possible multi-path propagation. The Oulu and Dortmund models predict significant lower values. With increasing distance, the prediction of both models improves. Up to a distance of 3 km the samples measured are found between the FSPL model and both coefficient models. In fact, the predicted values by the ITM model is more accurate up to this distance. However, the measured samples varies significant and a direct benefit of the terrain data is not visible in this plot.

For a deployment oriented comparison of the models, we implemented a binary classification for the FSPL model, the Oulu model, and the ITM model. Our binary classification splits the predictions into false positives and false negatives. False positives predictions are locations where the model predicts a connection to the gateway but there is none available. The false negatives describes the opposite prediction.

	ITM	FSPL	Oulu
False positive	12%	19%	5%
False negative	6%	0%	31%

TABLE III: Percentage share of false positives and false negatives.

The FSPL model generates 19% false positives, which would lead to possible sensor locations that are in fact not covered by the current gateway. False negatives are not present due to the overestimated RSSI. The Oulu model predicts only 5% false positive, but includes a huge number of false negative. The Oulu model (similar results were obtained for the Dortmund model) underestimates the possible RSSI. The ITM model leads to 12% false positive and 6% false negative. In Fig. 4, the distribution of the false positives and false negatives is shown on a map. In addition, we added a heatmap for each model to visualize the different RSSI predictions.

## VI. CONCLUSION AND FUTURE WORK

In this work, we tested different path-loss models for LoRa and compared the results to real measurements.

No perfect model is apparent from a comparison of the results. It is necessary to assess whether false positives or false negatives are more important for the deployment of a LPWAN. To ensure a signal reception, a reduction in false positives seems desirable, but may lead to unnecessary expenditures. A model with a balanced ratio of false positives and false negatives could be the correct choice. The ITM model generates this ratio and has the potential to significantly reduce this error at regions with huge elevation differences since

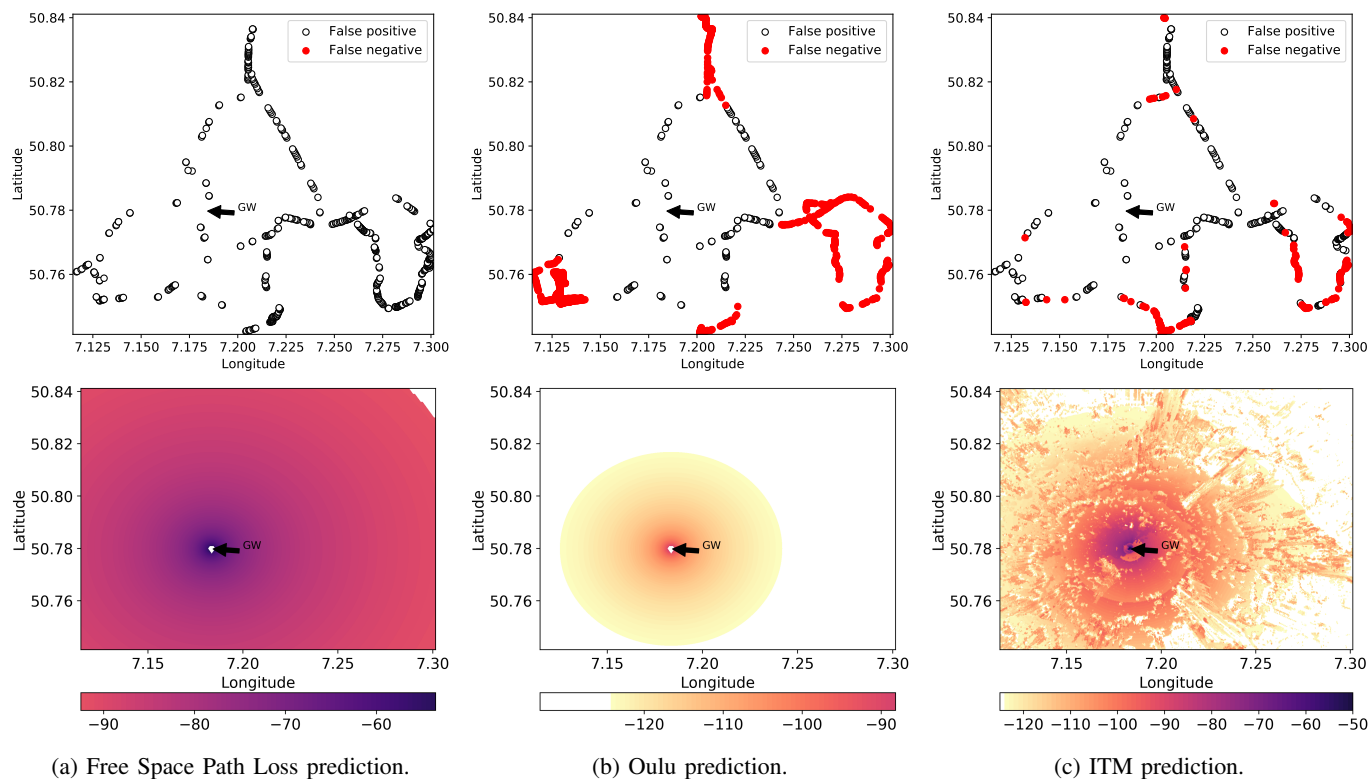


Fig. 4: Binary comparison and heatmaps for different path loss models.

especially mountains lead to many false negatives. Contrary to various publications in this area, we have demonstrated that the ITM model does not gratefully outperform other models for LPWAN but is especially useful in mountainous areas. We strongly assume that the accuracy could be increased by calculation reflections and diffraction for buildings or small terrain elevations more precisely using a LIDAR dataset. In 2017, the state of North Rhine-Westphalia made such a dataset (several terabyte) available online at [18]. Terrain data based path-loss modeling is commonly used and well-established for mobile radio or TV broadcasting. We have shown that the use of such data should be considered for LPWAN as well.

#### REFERENCES

- [1] Jörke *et al.*, “Urban channel models for smart city iot-networks based on empirical measurements of lora-links at 433 and 868 mhz,” in *2017 IEEE 28th Annual International Symposium on Personal, Indoor, and Mobile Radio Communications (PIMRC)*, Oct 2017, pp. 1–6.
- [2] Farhan *et al.*, “A survey on the challenges and opportunities of the internet of things (iot),” in *2017 Eleventh International Conference on Sensing Technology (ICST)*, Dec 2017, pp. 1–5.
- [3] Guibene *et al.*, “Evaluation of lpwan technologies for smart cities: River monitoring use-case,” in *2017 IEEE Wireless Communications and Networking Conference Workshops (WCNCW)*, March 2017, pp. 1–5.
- [4] A’ssri, Zaman, and Mubdi, “The efficient parking bay allocation and management system using lorawan,” in *2017 IEEE 8th Control and System Graduate Research Colloquium (ICSGRC)*, Aug 2017, pp. 127–131.
- [5] Lauridsen *et al.*, “Coverage comparison of gprs, nb-iot, lora, and sigfox in a 7800 km<sup>2</sup> area,” in *2017 IEEE 85th Vehicular Technology Conference (VTC Spring)*, June 2017, pp. 1–5.
- [6] (2018) Dhm-2007 terrain (10 m grid) and inspire\_tn roadlink. [Online]. Available: <https://download.kortforsyningen.dk/>
- [7] Petajajarvi *et al.*, “On the coverage of lpwans: range evaluation and channel attenuation model for lora technology,” in *2015 14th International Conference on ITS Telecommunications (ITST)*, Dec 2015, pp. 55–59.
- [8] “Bounding the Practical Error of Path Loss Models,” *Int. J. Antennas Propag.*, vol. 2012, pp. 1–21, 2012. [Online]. Available: <http://www.hindawi.com/journals/ijap/2012/754158/>
- [9] Friis, “A note on a simple transmission formula,” *Proceedings of the IRE*, vol. 34, no. 5, pp. 254–256, 1946.
- [10] Mikhaylov, “On the Coverage of LPWANs: Range Evaluation and Channel Attenuation Model for LoRa Technology,” pp. 55–59, 2016. [Online]. Available: [http://cc.oulu.fi/kmikhayl/site-assets/pdfs/2015\\_ITST.pdf](http://cc.oulu.fi/kmikhayl/site-assets/pdfs/2015_ITST.pdf)
- [11] Longley, Anita G and Rice, “Prediction of tropospheric radio transmission loss over irregular terrain. A computer method-1968,” Institute for telecommunication sciences boulder co, Tech. Rep., 1968.
- [12] Hufford, Longley, and Kissick, “A Guide to the Use of the ITS Irregular Terrain Model in the Area Prediction Mode,” *NTIA Tech. Rep. TR-82-100*, no. April, p. 126, 1982. [Online]. Available: <http://www.its.bldrdoc.gov/pub/ntia-rpt/82-100/>
- [13] Rabus *et al.*, “The shuttle radar topography mission a new class of digital elevation models acquired by spaceborne radar,” *ISPRS J. Photogramm. Remote Sens.*, vol. 57, no. 4, pp. 241–262, feb 2003. [Online]. Available: <http://linkinghub.elsevier.com/retrieve/pii/S1534580711002486>  
<http://linkinghub.elsevier.com/retrieve/pii/S0924271602001247>
- [14] (2018) Srtm data. [Online]. Available: <https://dds.cr.usgs.gov/srtm/version1/>
- [15] “SPLAT! A Terrestrial RF Path Analysis Application For Linux/Unix.” [Online]. Available: <http://www.qsl.net/kd2bd/splat.html>
- [16] Augustin *et al.*, “A study of lora: Long range i& low power networks for the internet of things,” *Sensors*, vol. 16, no. 9, 2016. [Online]. Available: <http://www.mdpi.com/1424-8220/16/9/1466>
- [17] (2018) Quectel l76-l. [Online]. Available: [http://www.quectel.com/UploadFile/Product/Quectel\\_L76-L\\_GNSS\\_Specification\\_V1.2.pdf](http://www.quectel.com/UploadFile/Product/Quectel_L76-L_GNSS_Specification_V1.2.pdf)
- [18] (2018) Opengedata nrw. [Online]. Available: <https://www.opengedata.nrw.de/produkte/geobasis/dom/dom11/>